

Quantum tunneling of vortices in two-dimensional condensates

Assa Auerbach,¹ Daniel P. Arovas,² and Sankalpa Ghosh^{3,*}

¹Physics Department, Technion, Haifa 32000, Israel

²Department of Physics, University of California at San Diego, La Jolla, California 92093, USA

³Physics Department, Okayama University, Okayama-700-8530, Japan

(Received 4 April 2006; revised manuscript received 13 June 2006; published 24 August 2006)

The tunneling rate t_v/\hbar of a vortex between two pinning sites (of strength \bar{V} separated by d) is computed using the Bogoliubov expansion of vortex wave-functions overlap. For BCS vortices, tunneling is suppressed beyond a few Fermi wavelengths. For Bose condensates, $t_v = \bar{V} \exp(-\pi n_s d^2/2)$, where n_s is the boson density. The analogy between vortex hopping in a superconducting film and two-dimensional electrons in a perpendicular magnetic field is exploited. We derive the variable range hopping temperature, below which vortex tunneling contributes to magnetoresistance. Using the “quantum Hall insulator” analogy we argue that the *Hall conductivity* (rather than the inverse Hall resistivity) measures the effective carrier density in domains of mobile vortices. Details of vortex wave functions and overlap calculations, and a general derivation of the Magnus coefficient for any wave function on the sphere, are provided in appendixes.

DOI: [10.1103/PhysRevB.74.064511](https://doi.org/10.1103/PhysRevB.74.064511)

PACS number(s): 03.75.Lm, 66.35.+a

I. INTRODUCTION

Mass and charge transport in superfluids, superconductors, and Bose Einstein Condensates (BEC) are governed by mobility of vortices.^{1,2} In two dimensions, vortex centers effectively interact as point charges in a perpendicular magnetic (Magnus) field. In the superfluid phase, vortices are pinned at zero temperature by impurity potentials.^{2,3} Their mobility, just below the pinning temperature scale, is dominated by thermally activated hopping,⁴ essentially following a classical Arrhenius law.

At lower temperatures, quantum fluctuations may, in principle, admit tunneling of vortices under energy barriers, resulting in “quantum flux creep.”⁵⁻⁷ Experimentally, vortex tunneling in superconducting films manifests itself as low temperature magnetization relaxation⁸ and nonactivated, variable range hopping resistivity.⁹ As magnetic field and disorder strength increase, vortex tunneling can turn into long range delocalization. This amounts to a quantum phase transition from the superfluid into an insulating,¹⁰⁻¹² or perhaps a Bose metal or vortex metal phase.¹³

A microscopic computation of vortex tunneling rates has been an elusive theoretical goal. The semiclassical (instanton) approach¹⁴ requires the determination of the “vortex mass” in the presence of Magnus dynamics, and low energy superfluid phonons.¹⁵⁻¹⁸

In the presence of short range, localized pinning potentials, it is simpler to compute (as we show below) the vortex tunneling rate from the many-body wave-function overlap.^{15,19-21}

In this paper we present a first detailed vortex overlap calculations for the following systems.

(i) *The weakly interacting Bose Einstein Condensate (BEC)*. The tunneling rate between two localized pinning potentials of strength \bar{V} , separated by distance d , is determined to be

$$t_v = \bar{V} \exp \left[-C \frac{\pi}{2} n_s d^2 + O(1/n_s \xi^2) \right], \quad (1)$$

where n_s and ξ are the boson number density and coherence length, respectively (see Fig. 1). Numerically $C=1 \pm 0.02$. The tunneling rate (1) applies to low density BEC’s and their charged version, the “Bosonic superconductor.” Equation (1) is computed using an antipodal vortex pair wave function on a spherical geometry (see Fig. 1).

(ii) *The BCS superconductor*. Conventional superconductors, with large electron density and core radius, have a tunneling rate which is suppressed by a factor of $e^{-0.2k_F^2 d^2}$, where k_F is the Fermi wave vector. Thus one can conclude that BCS

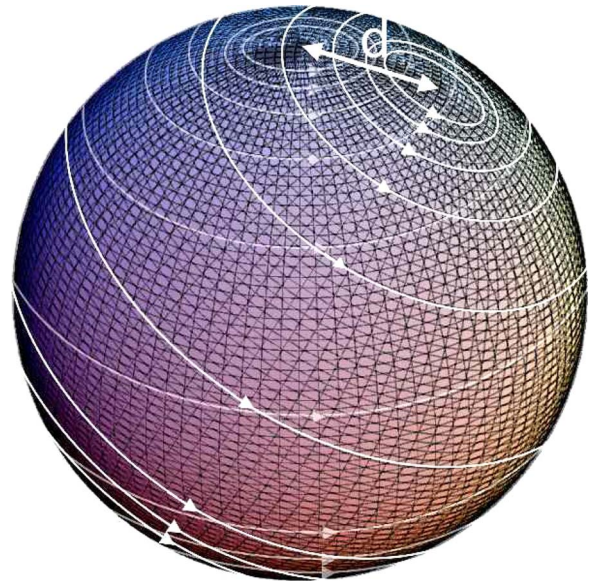


FIG. 1. (Color online) Overlap of two antipodal vortex-antivortex pair states on a sphere, shifted by distance d , which are used in this paper to numerically evaluate the vortex tunneling rate. White circles depict directions of circulating currents.

vortices cannot observably tunnel under barriers larger than a few Fermi wavelengths.

Our results point to the experimental regime where vortex tunneling in superconductors may have measurable effects on magnetotransport. Basically, the superfluid density should be much lower than the usual metallic electron density. This condition may be realized in cuprate (high T_c) films,⁸ especially in the underdoped regime,²² and in highly disordered superconducting films,^{11,12} where phase fluctuations are important.

The paper is organized as follows. Section II sets up the tunneling calculation by expressing the two site vortex tunneling rate in terms of the pinning energy and ground states overlap. Section III presents the overlap calculations of the interacting BEC [arriving at Eq. (1)], and the BCS superconductor. Section IV presents the vortex transport theory and its relation to electrical conductivity in superconductors. We use a quantum hopping Hamiltonian based on Eq. (1) coupled to the QED field of superfluid phonons.^{17,18} Following the theory of Ambegaokar, Halperin, and Langer²³ (AHL), we derive the variable range hopping exponent and temperature scale. The analogy to the “quantum Hall Insulator”^{24–26} is utilized to argue that the Hall *conductivity* of a bosonic superconductor is a robust measure of its boson number density n_s . (This is in contrast to the commonly used assignment of the “Hall number” using the inverse Hall *resistivity*.)

We provide pedagogically instructive details in a series of appendixes: the overlaps of vortex mean field state, in Appendix A, the Bogoliubov theory, in Appendix B, and Bogoliubov de-Gennes equations, in Appendix B 3, and their matrix formulations in the spherical geometry, in Appendix C.

In Appendix D we prove that the Magnus coefficient (adiabatic curvature) of an *arbitrary* wave function on the sphere is given by its average *angular momentum* density. This result, which is peripherally connected to the main subject of this paper, generalizes a previous proof connecting the vortex Magnus action to the far field density.²⁷

We conclude in Sec. V with a summary and a discussion.

II. VORTEX TUNNELING AND WAVE-FUNCTION OVERLAP

The relation between the vortex tunneling rate and wave-function overlap follows the method of nonorthogonal ground states first introduced by Heitler and London.²⁸

Let us consider a homogeneous condensate described by a many-body interacting Hamiltonian \mathcal{H}_0 . We perturb the system with two weak, and symmetrically situated, pinning sites at positions \mathbf{x}_1 and at \mathbf{x}_2 . The full Hamiltonian is

$$\mathcal{H} = \mathcal{H}_0 + \mathcal{V}_1 + \mathcal{V}_2, \quad (2)$$

where $\mathcal{V}_i = \lambda n(\mathbf{x}_i)$. The pinning potentials are repulsive for the bosons ($\lambda > 0$) and are therefore attractive for the vortices. The separation between the pinning sites is $d = |\mathbf{x}_2 - \mathbf{x}_1|$. We assume for this exercise that a reflection symmetry exists in \mathcal{H} about a mirror plane between the pinning sites. The ground states $|\Psi_i^0\rangle$ of the two *partial* Hamiltonians satisfy $(\mathcal{H}_0 + \mathcal{V}_i)|\Psi_i^0\rangle = E_0|\Psi_i^0\rangle$. Thus we can use the symmetric and

antisymmetric superpositions as variational ground states for the two symmetry sectors,

$$|\Psi_{\pm}^0\rangle = \frac{|\Psi_1^0\rangle \pm |\Psi_2^0\rangle}{\sqrt{2(1 \pm \langle \Psi_1^0 | \Psi_2^0 \rangle)}}. \quad (3)$$

Their corresponding energies are bounded by

$$E_{\pm}^0 \leq E_0 + \frac{\langle \Psi_1^0 | \mathcal{V}_2 | \Psi_1^0 \rangle \pm \langle \Psi_1^0 | \mathcal{V}_2 | \Psi_2^0 \rangle}{1 \pm \langle \Psi_1^0 | \Psi_2^0 \rangle}. \quad (4)$$

The coherent tunnel splitting is defined as $t_v = (E_+^0 - E_-^0)/2$. To first order in the overlap, $\langle \Psi_1^0 | \Psi_2^0 \rangle$, we obtain (see Ref. 29)

$$t_v \approx |\langle \Psi_1^0 | \mathcal{V}_2 | \Psi_1^0 \rangle \cdot \langle \Psi_1^0 | \Psi_2^0 \rangle - \langle \Psi_1^0 | \mathcal{V}_2 | \Psi_2^0 \rangle| \approx \bar{V} |\langle \Psi_1^0 | \Psi_2^0 \rangle|, \quad (5)$$

where $\bar{V} \equiv \langle \Psi_1^0 | \mathcal{V}_2 | \Psi_1^0 \rangle \approx \lambda n_1(\mathbf{x}_2)$. We neglect the term proportional to $\langle \Psi_1^0 | \mathcal{V}_2 | \Psi_2^0 \rangle$ since it depends on the density at the vortex center, which is assumed here to be small.

Thus Eq. (5) establishes that the pinning potential supplies the “attempt rate” of the tunneling. We shall see that the vortex wave-functions’ overlap depends primarily on the near field correlations, and decreases as a Gaussian of their separation d .

A. Overlap exponent and compressibility

We briefly review the important result of Niu, Ao, and Thouless (NAT)¹⁵ concerning vortex overlap. Consider a vortex centered at \mathbf{X} , with core radius ξ . The Onsager-Feynman³⁰ wave function is constructed from the uniform ground state Ψ_0 , and is therefore asymptotically correct for coordinates \mathbf{x}_i far from the core center.

$$\Psi_{\mathbf{X}} \approx \prod_i \{ \exp[i\phi(\mathbf{x}_i - \mathbf{X})] f(|\mathbf{x}_i - \mathbf{X}|/\xi) \} \Psi_0, \quad (6)$$

where $f(y) \rightarrow 1$ at $y \gg 1$. The overlap between two such wave functions, displaced by a distance d , is given by

$$\langle \Psi_{\mathbf{X}} | \Psi_{\mathbf{X}+d} \rangle = e^{-W_c} \exp\left(-\frac{\pi}{2} n_s d^2 \int_0^{\bar{k}} \frac{dk}{k} S(k)\right),$$

$$S(k) = \frac{1}{n_s} \int d^2\mathbf{x} \langle \Psi_0 | \delta n(0) \delta n(\mathbf{x}) | \Psi_0 \rangle e^{i\mathbf{k} \cdot \mathbf{x}}, \quad (7)$$

where W_c is the overlap of the core area. $\phi(\mathbf{x})$ is the angle between \mathbf{x} and the x axis. n_s is the average density, $\delta n = n - n_s$, and $\bar{k} \approx 2\pi/\xi$ is the core wave-vector cutoff.

The structure factor $S(k)$ is bounded by Bogoliubov’s inequality³¹

$$S(k) \leq \sqrt{F(k)\chi(k)}. \quad (8)$$

For interacting bosons of mass m and velocity independent interactions, the equal-time correlator F is given by

$$F(\mathbf{k}) \equiv \frac{\hbar^2}{N} \langle [n_{\mathbf{k}}, [H, \delta n_{-\mathbf{k}}]] \rangle = \frac{\hbar^2 k^2}{2m}. \quad (9)$$

The compressibility χ is related to the sound velocity c_s by

$$\lim_{k \rightarrow 0} \chi(k) \rightarrow \frac{1}{2mc_s^2}. \quad (10)$$

Inequality (8) ensures that for the interacting BEC, the momentum integration in Eq. (7) converges at low k , and therefore the vortex overlap exponent is finite in the thermodynamic limit.

We point out in Appendixes A and B 3 that both the Gross-Pitaevskii (mean field) coherent state and the BCS vortex wave functions suffer from a spurious overlap catastrophe, due to their unphysical, infinite compressibilities.³²

III. VORTEX OVERLAP CALCULATIONS

A. The interacting BEC

We consider a two-dimensional BEC with short range interactions, described by the second quantized Hamiltonian

$$\mathcal{H} = \int d^2x \left\{ \psi^\dagger K(\mathbf{A}) \psi + V(\mathbf{x}) \psi^\dagger \psi + \frac{g}{2} \psi^\dagger \psi^\dagger \psi \psi \right\}, \quad (11)$$

$\psi^\dagger(\mathbf{x})$ creates a boson of mass m and charge q at position \mathbf{x} ; μ is the chemical potential. The single particle potential $V(\mathbf{x})$ includes confining and vortex pinning contributions. The kinetic operator is

$$K(\mathbf{A}) = \frac{1}{2m} \left(\frac{\hbar}{i} \nabla + \frac{q}{c} \mathbf{A} \right)^2, \quad (12)$$

and \mathbf{A} is a vector potential. In the case of bosons of charge q in a magnetic field $\mathbf{B} = B\hat{z}$ and subject to a rotation $\boldsymbol{\omega} = \omega_{\text{rot}}\hat{z}$, the vector potential is $\mathbf{A} = (\frac{1}{2}B + mcq^{-1}\omega_{\text{rot}})\hat{z} \times \mathbf{x}$, and the single particle potential is shifted by $\Delta V(\mathbf{x}) = (\omega_{\text{rot}}/2c)(qB + mc\omega_{\text{rot}})\mathbf{x}^2$.

If the system is a uniform droplet of bulk density n_s , the chemical potential gets pinned at $\mu = gn_s$. The important parameters of the condensate are the phonon velocity $c_s = \sqrt{gn_s/m}$, and the coherence length is $\xi = \hbar/mc_s$.

We use boson coherent states (A1) to set up a semiclassical expansion of the partition function,

$$\begin{aligned} \mathcal{Z} &= \int \mathcal{D}[\varphi, \varphi^*] \exp \left\{ \int_0^{\hbar\beta} d\tau \int d^2x (i\varphi^* \partial_\tau \varphi - \mathcal{H}[\varphi^*, \varphi]) \right\} \\ &\approx \exp(-\beta E_{MF}[\bar{\varphi}]) \int \mathcal{D}[\eta, \eta^*] e^{-\mathcal{L}^{(2)}[\eta^*, \eta] + \mathcal{O}(\eta^3)}. \end{aligned} \quad (13)$$

The first exponential is the classical (mean field) energy, and the remaining path integral is over the fluctuation field $\eta = \varphi - \bar{\varphi}$.

The classical field $\bar{\varphi}$ minimizes the variational energy $\langle \varphi | \mathcal{H} | \varphi \rangle$. It solves the Gross-Pitaevskii (GP) equation^{33,34}

$$(K(\mathbf{A}) + V - \mu + g|\bar{\varphi}(\mathbf{x})|^2)\bar{\varphi}(\mathbf{x}) = 0. \quad (14)$$

With a weak pinning potential at the origin, and an external magnetic field or rotation,³⁵ a stable vortex solution can be found whose approximate analytic form is³⁶

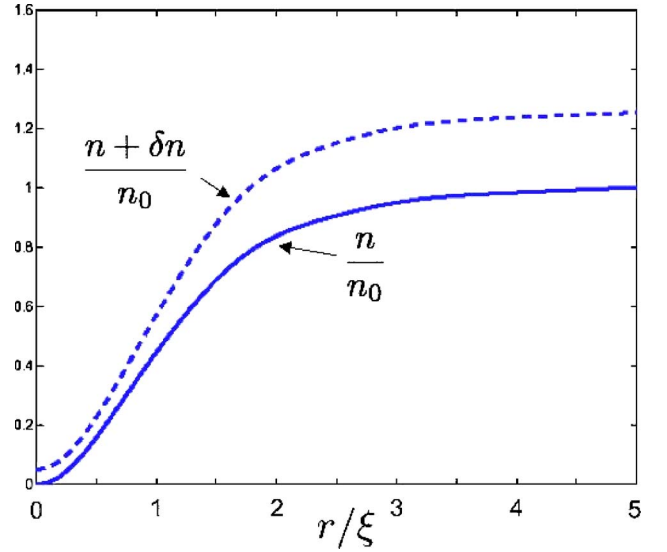


FIG. 2. (Color online) The mean field condensate density profile $n_0(r)$ corrected by the Bogoliubov fluctuations density $\delta n(r)$ as a function of radial distance r from the vortex center. n_0 is the far field asymptotic density.

$$\bar{\varphi} \approx \frac{\sqrt{n_0} r e^{i\phi}}{\sqrt{r^2 + \xi^2}}, \quad (15)$$

where (r, ϕ) are the polar coordinates of the vortex center, and n_0 is the mean field asymptotic condensate density. For numerical evaluation of the fluctuation spectrum, the trial solution (15) must be improved upon by iterating Eq. (14).

B. BEC vortex overlap

In Appendix A the mean field vortex coherent state is shown to suffer from an overlap catastrophe. In Appendix B, the Bogoliubov-fluctuations corrected ground state is given by

$$|\Phi\rangle = \mathcal{N} \exp\left(\frac{1}{2}\psi^\dagger Q \psi^\dagger\right) \exp(f\psi^\dagger)|0\rangle,$$

$$f(\mathbf{x}) \equiv \bar{\varphi}(\mathbf{x}) - \int d^2x' \bar{\varphi}^*(\mathbf{x}') Q(\mathbf{x}', \mathbf{x}), \quad (16)$$

where the operator Q is determined by solving Bogoliubov's equations. The density profile of $|\Phi\rangle$ is defined as

$$\delta n(\mathbf{x}) = \langle \Phi | n(\mathbf{x}) - n_0 | \Phi \rangle \quad (17)$$

and plotted in Fig. 2 as a function of radial direction from the vortex core.

The BEC vortex wave-function overlap is given by

$$|\langle \Phi_1 | \Phi_2 \rangle| = \exp(-W_0 - W_1). \quad (18)$$

We note that the leading order W_0 is proportional to the condensate density n_0 , while the fluctuation correction W_1 depends on d, ξ, R , but not on n_0 . $W_1(R)$ turns out to diverge logarithmically with system size R , which is simply an artifact of the Gaussian approximation in $|\Phi\rangle$. At this subleading order, in $1/(n_0\xi^2)$, the compressibility of this wave function

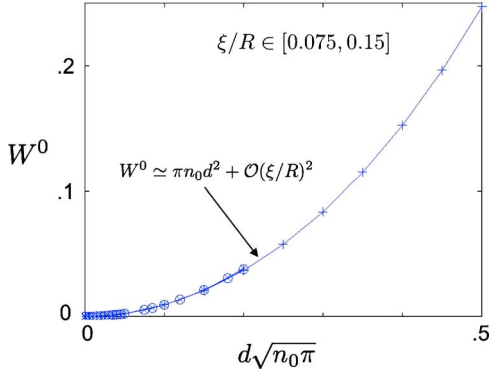


FIG. 3. (Color online) The leading order overlap exponent for an antipodal vortex pair of a BEC on a sphere, displaced by a distance d . n_0 is the mean field condensate density. Numerical data for Eq. (B16) are marked by crosses and circles representing different coherence lengths in the range $\xi/R \in [0.075, 0.15]$. The upper angular momenta cutoff was taken at $l_{\max}=60$. The solid line represents the fit with $C=1$ in Eq. (19).

diverges with R . However, this need not concern us here, since we limit our calculation to the leading order which has a finite compressibility.

In Appendix B we show that W_0 of Eq. (B17) is dominated by the core region. A numerical calculation, described in Appendix C, is used to determine $W(d, \xi)$. The numerical results for the antipodal vortex pair on a sphere of size R , depicted in Fig. 1, are presented in Fig. 3. An excellent analytical fit to the data is given by

$$W_0^{\text{sphere}}(d, R) = C \pi n_0 d^2 [1 + O(\xi/R)], \quad C = 1 \pm 0.02. \quad (19)$$

By halving the result for the vortex pair on a sphere [Eq. (19)], and taking the large R limit, we obtain the leading order result for a single vortex in the plane

$$W_0 = \frac{1}{2} \pi n_0 d^2 + O(\xi/R, \delta n), \quad (20)$$

which produces the result quoted in Eq. (1).

C. BCS vortex overlap

In Appendix B 3 the vortex wave-function overlap for an s -wave BCS superconductor is calculated by numerically solving Bogoliubov-de Gennes equations. Analysis of the far field contributions, combined with the numerical results yields

$$|\langle \Phi_1 | \Phi_2 \rangle| = \exp(-W^{\text{BCS}}),$$

$$W^{\text{BCS}} \simeq d^2 \left(\frac{k_F}{8\xi} \ln(R/\xi) + k_F^2 F(k_F \xi) \right), \quad (21)$$

where k_F is the Fermi wave vector, ξ is Pippard's coherence length and the vortex core size, and F is a dimensionless function of magnitude 0.2. The overlap catastrophe (logarithm of system size R) comes from the far field contributions and is an artifact of the infinite compressibility of the BCS wave function. The important lesson from Eq. (21) is

derived from the core region contribution $e^{-0.2k_F^2 d^2}$. This suppression is not affected by the long wavelength phase fluctuations, but arises from the large density of electrons in the Fermi sphere which change their momenta when the vortex moves. We can safely conclude therefore, that in high superfluid density superconductors, vortex tunneling cannot be observed beyond a distance of a few Fermi wavelengths.

IV. VORTEX TRANSPORT THEORY

Mobile vortices imply the destruction of the static superconducting order parameter. However, when order parameter (phase) correlations are of sizeable range, it is still convenient to describe the dissipative and Hall transport in terms of dilute vortices, rather than in terms of a dense system of interacting bosons. In two-dimensional BEC's, the neutral and charged BEC have analogous transport equations, since shielding can be ignored. The number current, pressure, and rotation frequency in the neutral BEC play the role of electrical current, voltage, and perpendicular magnetic field, respectively, in the bosonic superconductor. For convenience, we shall discuss the latter case, keeping a keen eye on possible experimental ramifications.

A. Vortex conductivity and electrical resistivity

Steady dissipative vortex motion can be driven by a bias current. For bosons with density n_s and charge q the current is $\mathbf{j}_c = q n_s \mathbf{v}_s$, where \mathbf{v}_s is the superfluid velocity. The vortex "charge" is the sign of its vorticity, $Q_v = \pm 1$, and the vortex "flux quantum" is a unit of boson particle number $\Phi_v^0 = 1$. The kinetic energy difference vortex at site \mathbf{R}_i and \mathbf{R}_j is

$$E_0(i) - E_0(j) = \frac{\hbar Q_v}{q} \mathbf{j}_c \times \hat{\mathbf{z}} \cdot (\mathbf{R}_i - \mathbf{R}_j). \quad (22)$$

The effective "electric" (actually *Magnus*) field acting on that vortex is

$$\boldsymbol{\varepsilon}_v = \frac{\hbar}{q} \mathbf{j}_c \times \hat{\mathbf{z}}. \quad (23)$$

The stable ground state of a charged superfluid (i.e., a superconductor) in a magnetic field B has a finite density of vortices given by

$$n_v = Bq/(hc), \quad (24)$$

where c is the speed of light. If the vortices have an average drift velocity \mathbf{V}_v the vortex current density is given by

$$\mathbf{J}_v = \frac{BqQ_v}{hc} \mathbf{V}_v. \quad (25)$$

The electromotive field (EMF) induced by the average vortex drift velocity is

$$\mathbf{E} = -c^{-1} \mathbf{V}_v \times \mathbf{B} = -\frac{\hbar}{q} \mathbf{J}_v \times \hat{\mathbf{z}}, \quad (26)$$

where c is the speed of light.

The "vortex conductivity" tensor is defined as σ_v ,

$$J_v^\alpha = \sum_\beta \sigma_v^{\alpha\beta} \epsilon_v^\beta. \quad (27)$$

Using Eqs. (23) and (25), the electric resistivity tensor ρ is directly related to the vortex conductivity by duality relations¹⁰

$$\begin{aligned} \rho^{xx} &= \left(\frac{\hbar}{q}\right)^2 \sigma_v^{yy}, & \rho^{yy} &= \left(\frac{\hbar}{q}\right)^2 \sigma_v^{xx}, \\ \rho^{xy} &= -\left(\frac{\hbar}{q}\right)^2 \sigma_v^{yx}. \end{aligned} \quad (28)$$

For example, consider unpinned vortices which can move in a Galilean invariant superfluid. The vortex Hall conductivity is given by analogy to a charged liquid of filling fraction ν , which is $\sigma^{xy} = \nu e^2/h$. Setting $e \rightarrow Q_v$, one obtains

$$\sigma_v^{xy} = \frac{Q_v}{h} n_v / n_s, \quad (29)$$

which by using Eqs. (24) and (28) yields (unsurprisingly) the classical electric Hall resistivity of a charged liquid with density n_s :

$$\rho_{\text{class}}^{xy} = -\frac{B}{n_s q c}. \quad (30)$$

This result will be used later, in Sec. IV D.

B. Vortex hopping Hamiltonian

Thus we arrive at a noninteracting vortex hopping Hamiltonian described by an Anderson tight binding model in a strong magnetic field

$$\mathcal{H}^v = \sum_i \epsilon_i c_i^\dagger c_i + \sum_{ij} t_v(d_{ij}) (e^{i\hbar \int_{x_i}^{x_j} dx \cdot \mathbf{a}} c_i^\dagger c_j + \text{H.c.}), \quad (31)$$

where c_i^\dagger creates a vortex at a random pinning site \mathbf{x}_i with random energy ϵ_i . \mathbf{a} is the Magnus gauge field which satisfies

$$\nabla \times \mathbf{a} = \hbar n_s \hat{\mathbf{z}}, \quad (32)$$

which gives rise to a Hall effect. The vortex hopping rate t_v was precisely defined by Eq. (5). For a weakly interacting BEC it was shown to decay with intersite separation d as a Gaussian

$$t_v(d) \sim \bar{V} \exp\left(-\frac{\pi}{2} n_s d^2\right). \quad (33)$$

The low energy vortex current operator is

$$\mathbf{J}_v(\mathbf{x}) = \frac{-i}{2\hbar} \sum_{ij} \mathbf{d}_{ij} t_v(d_{ij}) (c_j^\dagger c_i - \text{H.c.}) \delta(\mathbf{x} - \mathbf{x}_{ij}), \quad (34)$$

where \mathbf{d}_{ij} and \mathbf{x}_{ij} are the separation and midpoints of the pinning sites, respectively.

Vortex dynamics have been systematically derived for the two-dimensional translationally invariant superfluid using an effective quantum electrodynamics (QED) theory.^{17,18} In the QED formulation, vortices are point “charges,” moving in

the presence of a “transverse magnetic field” (the condensate density), and interacting with “photons” (the Bogoliubov phonons). The photons give rise to a vortex self-energy, which diverges logarithmically at low frequencies. This diverging “effective mass,” however, does not preclude quantum tunneling at finite time scales.³⁷

Following the derivation of Ref. 18, we explicitly retain the low energy phonons by coupling them as a gauge field to the vortex current:

$$\begin{aligned} \mathcal{H}^{v\text{-ph}} &= \int d^2x \mathbf{J}_v(\mathbf{x}) \cdot \mathbf{A}_\perp(\mathbf{x}) + \sum_{\mathbf{k}} \hbar c_s |\mathbf{k}| a_{\mathbf{k}}^\dagger a_{\mathbf{k}}, \\ \mathbf{A}_\perp &= \frac{i\hbar}{\sqrt{V}} \sum_{\mathbf{k}} e^{i\mathbf{k} \cdot \mathbf{x}} \left(\frac{n_s \xi}{2|\mathbf{k}|}\right)^{1/2} \hat{\mathbf{z}} \times \hat{\mathbf{k}} (a_{\mathbf{k}} + a_{-\mathbf{k}}^\dagger), \end{aligned} \quad (35)$$

where $a_{\mathbf{k}}^\dagger$ creates a Bogoliubov phonon (“photon” in the QED language¹⁸) of wave vector \mathbf{k} and frequency $\hbar c_s \mathbf{k}$, and $c_s = \hbar/(m\xi)$ is the speed of sound. The vortices are treated as hard-core particles, which like adsorbates on a surface, have a Fermi-Dirac occupation probability

$$n_i = (e^{(\epsilon_i - \mu)/T} + 1)^{-1}. \quad (36)$$

We set the chemical potential μ to zero and fix the average density $n_v = \sum_i n_i / N_{\text{pin}}$ by the magnetic field as given by Eq. (24). By inserting Eq. (34) in Eq. (35) for two sites separated by R , the two site conductance is given by the hopping theory (Ref. 38)

$$G^v(d) = \gamma_0 e^{-\pi n_s d^2} e^{-1/2T(|\epsilon_i| + |\epsilon_j| + |\epsilon_i - \epsilon_j|)} \quad (37)$$

where

$$\gamma_0 = \frac{2\pi n_v \bar{V}^2 d^4}{\hbar^4 T} \mathcal{R}^{\text{ph}}(\epsilon_i - \epsilon_j),$$

$$\begin{aligned} \mathcal{R}^{\text{ph}}(\omega) &= \text{Im} \int_{-\infty}^{\infty} dt e^{-i\omega t} \langle \mathbf{A}_\perp(\mathbf{x}, t) \mathbf{A}_\perp(\mathbf{x}, 0) \rangle \\ &= \frac{\hbar^2 n_s \xi}{4c_s} [1 + N_b(\omega/T)]. \end{aligned} \quad (38)$$

\mathcal{R}^{ph} is the bosons’ local dissipative response to the vortex motion, and N_b is the Bose function.

C. Vortex variable range hopping

The *macroscopic* vortex conductivity for the hopping Hamiltonian (31) requires knowledge of the distribution of pinning site positions and energies $\mathcal{P}(\{\mathbf{x}_i, \epsilon_i\})$. We focus our attention on *individual* vortex tunneling, in the regime of low vortex densities $n_v \ll n_{\text{pin}}$ and small random fluctuations $\delta\bar{V} \ll \bar{V}$. Interaction effects between vortices are self-consistently incorporated into ϵ_i .

The density of states depends on both the pinning potential distribution and the effects of vortex interactions. Here, we shall treat the low field, finite temperature regime where the mean hopping distance is much smaller than the vortex separation. The density of states is then reasonably modeled by

$$\mathcal{N}(\mathbf{x}, \epsilon) = \left\langle \sum_i \delta(\mathbf{x} - \mathbf{x}_i) \delta(\epsilon - \epsilon_i) \right\rangle = \frac{n_{\text{pin}}}{\delta\bar{V}}, \quad (39)$$

where n_{pin} is the pinning site density, and its energies are uniformly distributed in the interval $(-\delta\bar{V}/2, \delta\bar{V}/2)$.

The vortex conductivity maps onto Mott's variable range hopping (VRH)³⁹ of charges in a random potential and a strong magnetic field. The Gaussian decay of Eq. (33) is directly analogous to that of an electron in the lowest Landau level,^{40,41} where the ‘‘Landau length’’ is $\lambda = \sqrt{2\pi n_s}$.

At low enough temperatures $T < \delta\bar{V}$, there are typically many competing tunneling paths between pinning sites separated by distances $d \gg \lambda, 1/\sqrt{n_{\text{pin}}}$. As Shklovskii has shown,^{40,41} in this regime multiple (virtual) tunneling processes play a crucial role. Their primary effect is to replace the Gaussian decay of the two-site tunneling rate by a linear decay, typical of an Anderson insulator. Here, we must therefore replace $t_v(R)$ of Eq. (33) by

$$\tilde{t}_v \approx \bar{V} e^{-d/\ell}, \quad \ell = \frac{2s\sqrt{n_{\text{pin}}}}{\pi n_s}, \quad (40)$$

where ℓ is the linear localization length, and s is a pure number which depends on the details of $\mathcal{P}(\{\mathbf{x}, \epsilon\})$. Replacing Eq. (33) by Eq. (40), we arrive at a two-dimensional random resistor network of the kind discussed by Ambegaokar, Halperin, and Langer²³ (AHL), with random conductances given by

$$\tilde{G}_v^{ij} = \gamma_0 \exp\left(-\frac{2d_{ij}}{\ell} - \frac{|\epsilon_i| + |\epsilon_j| + |\epsilon_i - \epsilon_j|}{2T}\right). \quad (41)$$

By AHL, the macroscopic conductance is given by the critical (lowest) conductance G_v^c of the percolating subset of conductances which obey $\tilde{G}_{ij} \geq G_v^c$.

Taking the average number of bonds per site at percolation to be ν_c (e.g., on the square lattice $\nu_c = 2$), the percolating bonds all obey

$$\frac{2d_{ij}}{\ell} + \frac{|\epsilon_i| + |\epsilon_j| + |\epsilon_i - \epsilon_j|}{2T} \leq \ln(\gamma_0/G_v^c), \quad (42)$$

which can be written as

$$\frac{d_{ij}}{d_{\text{max}}} + \frac{|\epsilon_i| + |\epsilon_j| + |\epsilon_i - \epsilon_j|}{2\epsilon_{\text{max}}} < 1, \quad (43)$$

where

$$d_{\text{max}} = \frac{\ell}{2} \ln(\gamma_0/G_v^c), \quad (44)$$

$$\epsilon_{\text{max}} = T \ln(\gamma_0/G_v^c).$$

By Eq. (39) the density n_{conn} of connected sites within $|\epsilon_i| \leq \epsilon_{\text{max}}$ is given by

$$n_{\text{conn}} = n_{\text{pin}} \frac{\epsilon_{\text{max}}}{\delta\bar{V}}. \quad (45)$$

The percolation condition on the number of connections per site is

$$n_{\text{conn}} d_{\text{max}}^2 = \nu_c, \quad (46)$$

which implies the relation

$$\epsilon_{\text{max}} d_{\text{max}}^2 = \frac{\nu_c \delta\bar{V}}{n_{\text{pin}}}. \quad (47)$$

Using Eqs. (44) and (47) one obtains the value of the critical vortex conductance

$$G_v^c = \gamma_0 e^{-(T_0/T)^{1/3}},$$

$$T_0 = K \delta\bar{V} \left(\frac{\pi n_s}{n_{\text{pin}}}\right)^2, \quad (48)$$

where $K = 4\nu_c/s^2$ is a dimensionless factor of order unity. Using Eq. (28) we obtain the variable range hopping magnetoresistivity

$$\rho^{xx}(B, T) = \left(\frac{\hbar}{q}\right)^2 \gamma_0 [n_v(B)] e^{-(T_0/T)^{1/3}}. \quad (49)$$

$\rho^{xx}(B, T)$ exhibits vortex tunneling in two ways. First, the power of 1/3 in the exponential temperature dependence. Second, the VRH temperature scale T_0 depends strongly on the ratio of vortex tunneling length scales: the characteristic tunneling distance $1/\sqrt{n_{\text{pin}}}$ divided by the interboson separation $1/\sqrt{n_s}$.

At stronger fields (higher vortex density), long range vortex interactions are expected to modify the asymptotic power of the hopping exponent.⁹

D. Vortex Hall resistivity

1. Quantum Hall insulator: Review

Early on, Holstein⁴³ studied the Hall effect of the hopping model (31) at low temperatures. He has shown the importance of three site tunneling interference for producing a nonzero Hall effect.

Since then, several groups have extended that work to electrons in highly disordered two-dimensional semiconductors in the presence of a strong magnetic field.²⁴ Although different approximation schemes were used, these groups have concluded that while ρ^{xx} diverges at low frequency and temperature, $\lim_{\omega \rightarrow 0} \lim_{T \rightarrow 0} \rho^{xy}(\omega, T) < \infty$. Such behavior was dubbed ‘‘Quantum Hall insulator’’ (see Ref. 42).

Experiments in Hall bars⁴⁴ have found that the dc Hall resistivity has a much weaker temperature dependence than the resistivity on the insulator side of the field tuned metal-insulator transition. Reference 25 has remarkably found the Hall resistance in the insulator to be *quantized* at $h/e^2\nu$, at filling factor of $\nu = 1/3$.

The apparent difference between the behavior of the Hall resistance versus the longitudinal resistance can be explained

by Kirchoff's transport theory of an inhomogeneous resistor network,⁴⁵ with widely varying resistances. The Puddles Network Model (PNM)²⁶ was introduced to explain the experiments of Ref. 25. The PNM assumes a network of perfect Hall liquid puddles with conductivities $\sigma^{xy} = \nu e^2/h$, $\sigma^{xx} = 0$, embedded in an insulating environment and connected by arbitrary large, classical resistors. This model yields a quantized value of $\rho^{xy} = h/e^2\nu$, independent of ρ^{xx} .

While the PNM describes ohmic (incoherent) transport, quantum transport theory yields a different result. Using the Chalker-Coddington network to represent noninteracting electrons in the lowest Landau level in the presence of smooth disorder, Ref. 46 has numerically found that the Hall resistance at zero temperature actually diverges with system size, similarly to the quantum induced localization of ρ^{xx} . Therefore a true Hall insulator phase for the Chalker-Coddington model has been ruled out. The conflicting results of classical and quantum transport theories is related to the role of dephasing. Inelastic scattering destroys localization and prevents the divergence of ρ^{xy} .

2. Quantum vortex insulator

The above discussion is directly relevant to the vortex hopping model (31). The vortices are essentially in an insulating state with possible domains of weaker superconductivity where vortex mobility is higher. A diverging σ^{xy} at low temperatures may indicate long range coherent vortex transport, an interesting result in itself.

Let us for now assume sufficient dephasing at the low temperature of experiments, due to vortex-phonon, or vortex fermion interactions. We can appeal to the Boltzmann transport theory and to the resistor network models. This implies that the Hall *conductance* (not resistance) is determined by the Hall conductivity σ^{xy} of the most "insulating" puddles. We do not know how to compute the distribution of σ^{xy} . However, by Eq. (29), σ^{xy} measures the effective carrier density n^* in the most resistive domains (i.e., the vortex liquid puddles):

$$\sigma^{xy}(B) \sim n_s^* q c / B. \quad (50)$$

Furthermore, a detection of "quantized" plateaus of $\sigma^{xy}(B, n_s)$ may indicate locked-in charge density waves or topological ordering⁴⁸ in the vortex-condensed domains.

V. EXPERIMENTAL IMPLICATIONS AND DISCUSSION

BEC of cold atoms. Vortices have been created in rotating cold atomic gases.⁴⁹ One can imagine optically introducing localized pinning potentials and measuring the excitation spectrum. The lowest antisymmetric excitation could be compared to expression (1) for different potential separations and boson densities.

Cuprate superconductors. In thin cuprate films, time resolved magnetization relaxation⁸ is a direct measure of the average vortex mobility. A variable range hopping behavior of the magnetoresistance section is indicative of tunneling effects, as was shown in Sec. IV C. For a "bosonic supercon-

ductor" (coupled only to order parameter phase fluctuations), the characteristic resistivity given in Eq. (49) is

$$\frac{h^2}{q^2} \gamma_0 \sim \frac{h}{q^2} \left(\frac{n_v}{n_{\text{pin}}} \right) \left(\frac{\bar{V}}{T} \right) \left(\frac{n_s}{n_{\text{pin}}} \right) n_s \xi^2. \quad (51)$$

This expression has dubious applicability to high T_c films. However, if one accepts a model of tightly bound hole pairs, with a low superfluid density, the vortices can primarily dissipate momentum to the low energy "nodal" fermions, and the core states near the vortex center.^{50,51} Incorporating general fermionic excitations (which could also be induced by short range disorder) can be achieved by including a dissipative response to \mathcal{R}^{ph} , given by

$$\mathcal{R}^{\text{fer}}(\omega) = \left(\frac{h^2 c^2}{e^2 \omega} \right) \sigma^{\text{ferm}}(\omega), \quad (52)$$

where $\sigma^{\text{ferm}}(\omega)$ is the fermions contribution to the ac conductivity. Crudely estimating the factors contributing to the characteristic resistivity, we obtain

$$\frac{h^2}{q^2} \gamma_0 \sim \frac{h}{q^2} \left(\frac{n_v}{n_{\text{pin}}} \right) \left(\frac{\bar{V}}{T} \right) \left(\frac{\bar{V}}{\delta \bar{V}} \right) \left(\frac{\sigma(\delta \bar{V}/\hbar)}{e^2/h} \right). \quad (53)$$

The values of \bar{V} and $\delta \bar{V}$ may be extracted from the resistance activation energy at higher temperatures. Nikolic and Sachdev⁵² have recently considered the effects of nodal fermions on the vortex dynamics in a charged d -wave superconductor. They have found that only a finite vortex mass renormalization is induced, and a viscous drag term which rises with temperature as T^2 .

Hall conductivity. Hall effect measurements in underdoped cuprates have determined the Hall number as $n_H(T) = -B/(\rho^{xy} e c)$ and found it to be of the same sign and magnitude as the *hole* doping concentration away from the Mott insulator phase.⁵³ However, the "anomalous" strong temperature dependence of $n_H(T)$ has been used to distinguish the unconventional nature of the cuprates which differs from the much weaker temperature dependence of the Hall number in conventional metals.

Our analysis suggests that the Hall conductivity, Eq. (50), rather than Hall resistivity, should be used to define a Hall number in the superconducting phase. In this regime, accessible by strong magnetic fields,⁵⁴ σ^{xy} is expected to be less temperature dependent and to characterize the Hall coefficient of metallic "puddles" inside the superconductor, where vortices are locally delocalized by tunneling.

Disordered superconducting films. Highly disordered superconducting films¹¹ are also likely candidates for observing vortex tunneling since they effectively exhibit low superfluid density. We expect variable range hopping and a finite Hall conductivity near the superconductor-insulator transition, where vortices become delocalized. However, we refrain from quantitative estimates for these effects since a microscopic theory for strongly inhomogeneous interacting fermion systems is beyond the scope of this paper.

Periodic lattices. Optical lattices of cold bosons and Josephson junction arrays introduce the challenge of a strong periodic potential. The vortex hopping Hamiltonian (31) can

describe a periodic lattice of weak pinning potentials. One expects the lattice constant to play an important role in vortex mobility. The analogous Hofstadter problem⁴⁷ of a tight binding electron motion in a strong magnetic field demonstrates the strong effects of commensurability between the site and flux quanta densities. Indeed, recent theoretical work has shown⁴⁸ that ground states degeneracies and vortex dynamics depend on the boson filling per lattice site.

ACKNOWLEDGMENTS

We thank Ehud Altman and Anatoli Polkovnikov for correcting an erroneous conclusion in an earlier version of this work.³² Conversations with S. Gayen, M. Fogler, A. Kapitulnik, A. Keren, S. Kivelson, D.-H. Lee, A. Mizel, E. Shimshoni, E. Sonin, Z. Tesanovic, and O. Vafeek are gratefully acknowledged. We acknowledge support from the US-Israel Binational Science Foundation and the fund for promotion of research at Technion. We are grateful for the hospitality of Aspen Center for Physics, Kavli Institute for Theoretical Physics and Lewiner Institute for Theoretical Physics at Technion, where portions of this research were carried out.

APPENDIX A: SPURIOUS OVERLAP CATASTROPHE IN MEAN FIELD THEORY

This appendix provides pedagogical examples which reflect the limitations of mean field theory of superfluids of superconductors. In particular, we show that Bose coherent states and Bogoliubov de-Gennes wave functions have logarithmically divergent overlap exponents in the thermodynamic limit, as a consequence of their infinite compressibilities.

1. Bose coherent states

Coherent states wave functions are often used as zeroth order approximations to ground states of Bosons, superconductors, and quantum spin models with long range order. Here we show that when describing a vortex, coherent states generically exhibit an overlap catastrophe, i.e., a logarithmically diverging exponent. This divergence is an artifact of the unphysical infinite compressibility exhibited by noninteracting bosons.

Consider the coherent state $|\varphi\rangle$, with $\varphi = \sqrt{n_0}e^{i\phi}$ a complex scalar field, defined by

$$|\varphi\rangle = \exp \int d^2x (\varphi(\mathbf{x}) \psi^\dagger(\mathbf{x}) - \varphi^*(\mathbf{x}) \psi(\mathbf{x})) |0\rangle. \quad (\text{A1})$$

The overlap exponent between two translated vortex coherent states (A1), centered at $\mathbf{X} = \pm \frac{1}{2} \mathbf{d}$ is then $|\langle \varphi_1 | \varphi_2 \rangle| = \exp(-W^{\text{CS}})$, with

$$W^{\text{CS}} = \int d^2x \left[\frac{1}{2} (|\varphi_1|^2 + |\varphi_2|^2) - \text{Re} \varphi_1^* \varphi_2 \right].$$

The far field integral (away from the core) $n_i(\mathbf{x}) \approx n_0$. In this case, $\varphi \sim \sqrt{n_0} \exp(i\phi)$, where ϕ is the angle function relative to the vortex center (see Fig. 4).

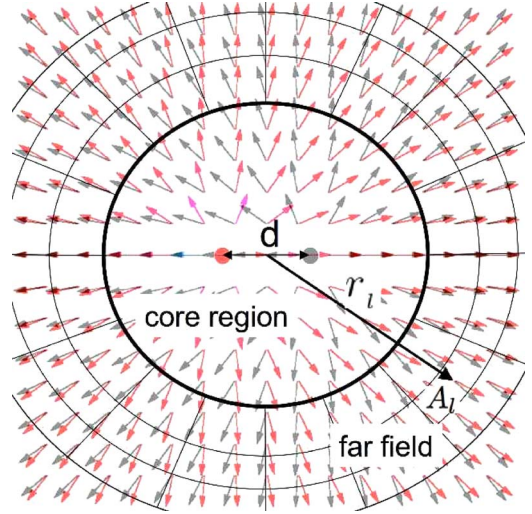


FIG. 4. (Color online) Overlap of two vortex coherent states as described by Eq. (A2). Black (red) arrows are vector representations of φ_1 (φ_2). For asymptotic calculations of BEC and BCS cases, see Eqs. (B17) and (B29), the far field region is divided into uniform phase blocks labeled by l at distances r_l and areas A_l .

$$\begin{aligned} W_{\text{far}}^{\text{CS}}(d) &= n_0 \int_{r_0}^R d^2x [1 - \cos(\phi_1 - \phi_2)] \\ &\approx \frac{1}{2} n_0 \int_{r_0}^R d^2x \left(\frac{\mathbf{d} \cdot \nabla \phi}{r} \right)^2 \\ &= \frac{1}{2} \pi n_0 d^2 \ln(R/r_0), \end{aligned} \quad (\text{A2})$$

where r_0 is a near field cutoff. This calculation was first presented by Sonin¹⁹ in the context of vortex tunneling using a noninteracting (product) condensate wave function.

For the noninteracting Bose condensate wave function, it is easy to verify that the structure factor is

$$\langle \delta n(\mathbf{x}) \delta n(\mathbf{x}') \rangle = \delta(\mathbf{x} - \mathbf{x}') n_0 \quad (\text{A3})$$

which yields finite zero momentum density fluctuations $\lim_{k \rightarrow 0} S^{\text{CS}}(k) = T \chi = 1$. This is an artifact of the unphysical limit of *noninteracting* bosons, where the sound velocity vanishes and the compressibility $\chi(T=0)$ is infinite. The wave-function overlap integral in Eq. (7) diverges logarithmically with the lower momentum cutoff, signaling this orthogonality catastrophe seen in Eq. (A2). Recall, however, that noninteracting bosons do not support stable vortices as their coherence length is infinite.

APPENDIX B: BOGOLIUBOV FLUCTUATIONS

The fluctuations η in Eq. (13) are governed by the harmonic action

$$S^{(2)} = \frac{1}{2} \int d\tau \int d^2x (\eta^* \eta) [iJ \partial_\tau - H^{(2)}] \begin{pmatrix} \eta \\ \eta^* \end{pmatrix}, \quad (\text{B1})$$

where

$$J \equiv \begin{pmatrix} 1 & 0 \\ 0 & -1 \end{pmatrix}, \quad H^{(2)} = \begin{pmatrix} H_0 & g\tilde{\varphi}^2 \\ g\tilde{\varphi}^{*2} & H_0^* \end{pmatrix}, \quad (\text{B2})$$

and $H_0 = K(\mathbf{A}) + 2g|\tilde{\varphi}(\mathbf{x})|^2 - \mu$.

The Hamiltonian $H^{(2)}$ is diagonalized by the canonical transformation,

$$S = \begin{pmatrix} U & V^* \\ V & U^* \end{pmatrix}, \quad S^\dagger H^{(2)} S = \begin{pmatrix} \hat{E} & 0 \\ 0 & \hat{E} \end{pmatrix}, \quad (\text{B3})$$

with

$$S^\dagger \hat{J} S = \hat{J} = S \hat{J} S^\dagger. \quad (\text{B4})$$

Here we use the Dirac matrix notations for the eigenfunctions,

$$\langle \mathbf{x} | U | n \rangle = U_n(\mathbf{x}),$$

$$\langle \mathbf{x} | V | n \rangle = V_n(\mathbf{x}). \quad (\text{B5})$$

The spectrum is given by the diagonal matrix $\langle n | \hat{E} | n \rangle = \delta_{nn'} E_n$.⁵⁵ The Bogoliubov eigenoperators and spectrum are determined by solving the differential equations,

$$\begin{aligned} H_0 U_n(\mathbf{x}) + g\tilde{\varphi}^2 V_n(\mathbf{x}) &= +E_n U_n(\mathbf{x}), \\ g\tilde{\varphi}^{*2} U_n(\mathbf{x}) + H_0^* V_n(\mathbf{x}) &= -E_n V_n(\mathbf{x}), \end{aligned} \quad (\text{B6})$$

1. Bogoliubov corrections in the far field approximation

In a large area, asymptotically far away from the vortex core, we can solve the Bogoliubov equations (B6) using a constant order parameter, $\tilde{\varphi} = \sqrt{n_0} e^{i\phi}$. $H^{(2)}$ is diagonal in Fourier space, and the matrix Q is given by

$$\langle \mathbf{k} | Q | \mathbf{k}' \rangle = -\frac{e^{2i\phi}}{\mu} [\varepsilon_k - \mu - E(\varepsilon_k)] \delta_{\mathbf{k}, \mathbf{k}'} \equiv e^{2i\phi - \theta_k} \delta_{\mathbf{k}, \mathbf{k}'}, \quad (\text{B7})$$

where $\varepsilon_k = \hbar^2 k^2 / 2m$ and $E(\varepsilon) = \sqrt{\varepsilon^2 + 2\mu\varepsilon}$. The Bogoliubov fluctuations lead to an increase in the density. Defining $\delta n = n_s - n_0$,

$$\begin{aligned} \delta n &= \langle \Phi | \eta^\dagger \eta | \Phi \rangle = \frac{1}{2} \sum_k v^2(\varepsilon_k), \\ v^2(\varepsilon) &= \frac{\mu^2}{2\sqrt{(\varepsilon + \mu)^2 - \mu^2}(\varepsilon + \mu + \sqrt{(\varepsilon + \mu)^2 - \mu^2})}, \end{aligned} \quad (\text{B8})$$

and changing variables to $y = 1 + \varepsilon/\mu$, one obtains

$$\delta n = \frac{1}{\pi \xi^2} \int_1^\infty \frac{dy}{2\sqrt{y^2 - 1}(y + \sqrt{y^2 - 1})} = \frac{1}{4\pi \xi^2}. \quad (\text{B9})$$

The dimensionless parameter which controls the higher order terms in the saddle point expansion of Eq. (13) is then $\delta n/n_0 = 1/(4\pi n_0 \xi^2)$, which serves as an effective ‘‘quantum disorder’’ coupling constant.

For a uniform condensate, the leading order structure factor is given by

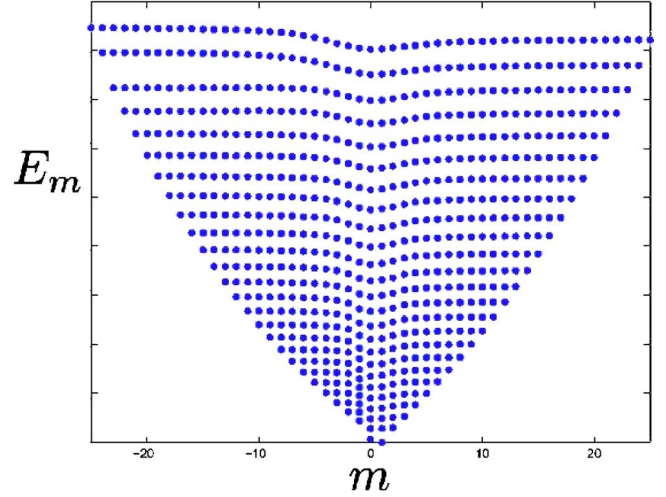


FIG. 5. (Color online) The exact Bogoliubov spectrum for a vortex pair configuration on the sphere, as a function of azimuthal quantum number m . The relevant parameters are $\xi/R=0.1$, and a stabilizing rotation frequency of $\omega_{\text{rot}}=1.875\hbar/mR^2$. Note the non-degenerate zero mode at $m=1$. Note the vortices induced distortion of the spectrum around $m \approx 0$ in a broad energy range.

$$S^{\text{Bog}} = \frac{\varepsilon_q}{E_q} + O(n_0 \xi^2)^{-1}, \quad (\text{B10})$$

where the order $1/(n_0 \xi^2)$ corrections go beyond the leading order approximation and hence are ignored. An artifact of the wave function Φ , in Eq. (16), is that it produces a nonvanishing contribution at zero momentum (i.e., an infinite compressibility) from the fluctuations correlator $\langle \Phi | (\eta)^4 | \Phi \rangle$. These should be cancelled at this (subleading) order in $1/(n_0 \xi^2)$, by self-energy corrections due to cubic interactions $g\tilde{\varphi}^* \eta^*(\eta)^2$, which we will not calculate here.

A quantum phase transition into another zero temperature phase (e.g., a solid) may be expected when $\delta n \gtrsim n_0$. Here we shall not explore the strong coupling regime.

2. Full vortex Bogoliubov theory

In Fig. 5 the numerical fluctuation spectrum about a vortex pair configuration on a sphere is plotted as a function of angular momentum. Equation (14) has a zero mode⁵⁶ ($E_n = 0$) corresponding to a global U(1) phase transformation $\phi \rightarrow \phi + \delta$, given by

$$U_0(\mathbf{x}) = A\tilde{\varphi}(\mathbf{x}), \quad V_0(\mathbf{x}) = A^* \tilde{\varphi}^*(\mathbf{x}),$$

$$\int d^2x (|U_0|^2 - |V_0|^2) = 0. \quad (\text{B11})$$

This (unnormalizable) zero mode, which enforces charge conservation, is henceforth excluded from our numerical spectra.

The Bogoliubov eigenoperators (quasiparticles) are given by

$$a_n = \int d^2x (U_n^*(\mathbf{x}) \eta(\mathbf{x}) - V_n^*(\mathbf{x}) \eta^*(\mathbf{x})). \quad (\text{B12})$$

To visualize the Bogoliubov fluctuations near a vortex, we plot in Fig. 6 the tunneling density of states as defined by

$$T(E, \mathbf{x}) = \pi \sum_n |V_n(\mathbf{x})|^2 \delta(E - E_n), \quad (\text{B13})$$

which might prove interesting for inelastic scattering experiments of rotating condensates.⁵⁷

The Bogoliubov corrected ground state $|\Phi\rangle$ is the a -vacuum, and thus satisfies $a_n|\Phi\rangle=0$. This may be written in terms of the original bosons as

$$\begin{aligned} |\Phi\rangle &= \mathcal{N} \exp\left(\frac{1}{2} \int d^2x d^2x' \psi^\dagger(\mathbf{x}) Q(\mathbf{x}, \mathbf{x}') \psi^\dagger(\mathbf{x}')\right) \\ &\times \exp\left(\int d^2x f(\mathbf{x}) \psi^\dagger(\mathbf{x})\right) |0\rangle \\ f(\mathbf{x}) &\equiv \tilde{\varphi}(\mathbf{x}) - \int d^2x' \tilde{\varphi}^*(\mathbf{x}') Q(\mathbf{x}', \mathbf{x}). \end{aligned} \quad (\text{B14})$$

Integration over coordinates is implied in Eq. (B14), and the normalization factor is $\mathcal{N} = \langle \Phi | \Phi \rangle^{-1/2}$. The pair operator Q is given by

$$Q(\mathbf{x}, \mathbf{x}') \equiv \langle \mathbf{x} | (U^\dagger)^{-1} (1 - |0\rangle\langle 0|) V^\dagger | \mathbf{x}' \rangle = Q(\mathbf{x}', \mathbf{x}), \quad (\text{B15})$$

where the matrices U^\dagger and V were defined in Eq. (B5). The zero mode (B11) denoted by $|0\rangle$, is projected out in Eq. (B15) as required by Bogoliubov's saddlepoint expansion. In the following we shall compute the operator Q in convenient bases.

We next compute the overlap of a vortex state with a displaced vortex. For two vortex states (16) centered at \mathbf{X}_i , $i=1, 2$, the operators $Q_i(\mathbf{x}, \mathbf{x}')$ are distinct and not translationally invariant. The magnitude of the wave-function overlap for Bogoliubov-corrected vortex states is

$$\begin{aligned} |\langle \Phi_1 | \Phi_2 \rangle| &= \exp(-W_0 - W_1), \\ W_0 &= W_0^{(12)} - W_0^{(11)}, \quad W_1 = -\ln \left| \frac{D_{12}}{D_{11}} \right|, \\ W_0^{(ij)} &= \frac{1}{2} (f_i^* f_j) \begin{pmatrix} 1 & -Q_j \\ -Q_i^* & 1 \end{pmatrix}^{-1} \begin{pmatrix} f_j \\ f_i^* \end{pmatrix}, \\ D_{ij} &= \det^{-1/2} (1 - Q_i^* Q_j). \end{aligned} \quad (\text{B16})$$

We note that the leading order W_0 is proportional to the condensate density n_0 , while the fluctuation correction W_1 depends on d, ξ, R , but not on n_0 . W_1 turns out to diverge logarithmically with system size. However, in this paper we avoid calculating the subleading order corrections, since we know that at the same order, the structure factor of Φ is incomplete, as discussed after Eq. (B10).

We now show that in contrast to the coherent state overlap result (A2), there is no logarithmic divergence, to leading order, in the exponent $W_0(d, R)$. This can be shown analytically by separating contributions of the core and the far field regions, as depicted in Fig. 4,

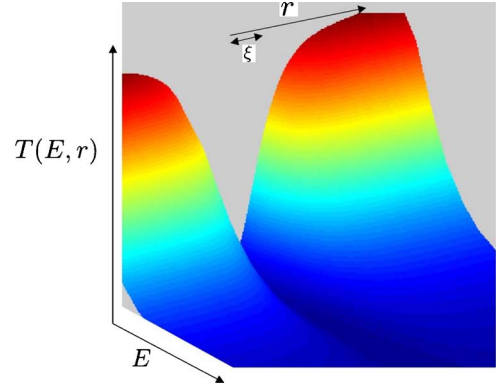


FIG. 6. (Color online) The Bogoliubov tunneling density of states of a BEC vortex (in arbitrary units) as a function of excitation energy E and radial distance from the vortex center r . ξ is the coherence length.

$$W^0 \sim \int_{\text{core}} d^2x w_{\text{core}}(\mathbf{x}) + \sum_l A_l w_{\text{far}}(\mathbf{x}_l). \quad (\text{B17})$$

The far field integral is approximated by a sum over constant phase domains, at radii $r_l \gg \xi$, and of areas $A_l \ll r_l^2$, corresponding to the condensate field $\varphi_{i,l} = \sqrt{n_0} \exp(i\phi_{i,l})$. We use the uniform solutions (B7) in each such domain, assuming that the block sizes are large enough: $A_l \gg \xi^2$. Thus

$$Q_{i,l} = -\frac{e^{2i\phi_{i,l}}}{A_l} \sum_{k \neq 0} Q_k e^{ik \cdot (\mathbf{x} - \mathbf{x}')} = -e^{i2\phi_{i,l}} (\delta(\mathbf{x} - \mathbf{x}') + O(\xi/r_l)), \quad (\text{B18})$$

which, by Eq. (16), yields in each block l , and vortex configurations $i=1, 2$, the constant functions

$$\begin{aligned} f_{i,l}(\mathbf{x}) &= \sqrt{n_0} \left(e^{i\phi_{i,l}} - e^{-i\phi_{i,l}} \int_l d^2x' Q_{i,l}(\mathbf{x}, \mathbf{x}') \right) \\ &= 2\sqrt{n_0} e^{i\phi_{i,l}} + O(\xi/R). \end{aligned} \quad (\text{B19})$$

Using Eq. (B16) we obtain to zeroth order in ξ/r_l the result

$$\begin{aligned} w_{\text{far}}(\mathbf{x}_l) &\simeq n_0 \text{Re} \left\{ \left(e^{-i\phi_1} e^{i\phi_2} \right) \frac{\begin{pmatrix} 1 & -e^{i2\phi_2} \\ -e^{-i2\phi_1} & 1 \end{pmatrix}}{1 - e^{i2(\phi_2 - \phi_1)}} \right. \\ &\quad \left. \times \left(\begin{pmatrix} e^{i\phi_2} \\ e^{-i\phi_1} \end{pmatrix} - (\phi_2 \leftrightarrow \phi_1) \right) \right\} \\ &= 4n_0 \text{Re} \left(\frac{e^{i(\phi_2 - \phi_1)}}{1 + e^{i(\phi_2 - \phi_1)}} - \frac{1}{2} \right) = 0, \end{aligned} \quad (\text{B20})$$

where we have suppressed the block index l . Unlike in the coherent states overlap exponent which exhibits a logarithmic divergence (A2), W_0 is perfectly finite in the large system limit

$$\sum_l A_l w_l^{\text{far}} = \int_{r_0}^{\infty} d^2r (\mathbf{d} \cdot \nabla \phi)^2 \times O(\xi/r) < \infty \quad (\text{B21})$$

which is in agreement with NAT (7) and (B10).

3. Vortex overlap in BCS states

It is perhaps little appreciated in the literature that vortex wave functions of BCS theory of superconductors, as derived by leading order Bogoliubov de-Gennes equations, suffer from the same *overlap orthogonality catastrophe* and infinite compressibility as the Bose coherent states described above.

We shall demonstrate this point by considering a “generic” BCS superconductor, which is described by a microscopic Hamiltonian of attractively interacting fermions:

$$\mathcal{H} = \int d^2x \left\{ \psi_s^\dagger (K + V) \psi_s - \frac{g}{2} \psi_s^\dagger \psi_{s'}^\dagger \psi_{s'} \psi_s \right\},$$

where $\psi_s(\mathbf{x})$ creates an electron of mass m , charge q , and spin $s = \uparrow, \downarrow$ at position \mathbf{x} , and the operators of kinetic (K) and potential (V) energy are the same as defined for bosons in Eqs. (12) and (11), and we similarly use the Dirac matrix notation for operators and vector notation for functions. Summation over repeated spin indices s, s' is assumed. The complex superconducting order parameter is $\varphi(\mathbf{x}) = \langle \psi_\uparrow(\mathbf{x}) \psi_\downarrow(\mathbf{x}) \rangle$. At long distances from the edges or vortex cores, φ minimizes the Ginzburg-Landau energy, i.e., it satisfies Gross Pitaevskii equation (14) with pair mass $2m$ and charge $q=2e$. Its magnitude is given by the BCS gap parameter, i.e., $\Delta = g|\varphi|$. As for the BEC, in the presence of a weak magnetic field, a quantized vortex solution minimizes the mean field energy, and its core size is given by the coherence length $\xi \simeq \hbar v_F / \pi \Delta_0$, where v_F is the Fermi velocity.²

The Bogoliubov de-Gennes (BdG) equations for the superconductor are

$$H_0 U_n(\mathbf{x}) + g \varphi V_n(\mathbf{x}) = E_n U_n(\mathbf{x}),$$

$$g \varphi^* V_n(\mathbf{x}) - H_0^* U_n(\mathbf{x}) = E_n V_n(\mathbf{x}),$$

where $H_0 = K - \mu$ and $\mu = \hbar^2 k_F^2 / 2m$, along with the self-consistency condition

$$\sum_n U_n(\mathbf{x}) V_n^*(\mathbf{x}) = \varphi(\mathbf{x}). \quad (\text{B22})$$

The self-consistency determines the detailed profile of $|\varphi(\mathbf{r})|$ in the core region. The exact BdG spectrum of the vortex pair on the sphere is depicted in Fig. 7.

Using the solutions of Eq. (B22) the two vortex ground states are given by

$$|\Phi\rangle_i = \mathcal{N} \exp(\psi_i^\dagger Q_i \psi_i) |0\rangle, \quad i = 1, 2,$$

$$Q_i = \langle \mathbf{x} | (U_i^\dagger)^{-1} V_i^\dagger | \mathbf{x}' \rangle, \quad (\text{B23})$$

where \mathcal{N} is the normalization. The normalized overlap of two BCS vortex states displaced by \mathbf{d} is given by

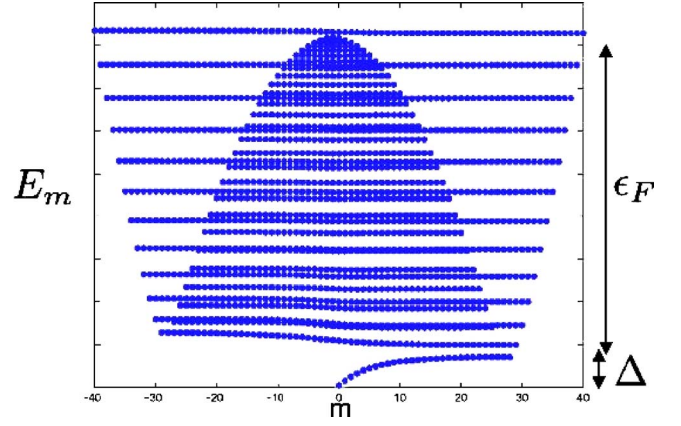


FIG. 7. (Color online) The Bogoliubov-de Gennes spectrum for a vortex pair configuration on the sphere, as a function of azimuthal quantum number m . The relevant parameters are the BCS gap Δ and the Fermi energy ϵ_F . Note the branch of (doubly degenerate) low energy Caroli-de Gennes-Matricon core states at positive angular momenta.

$$e^{-W(d)} = \frac{|\det(1 + Q_1 Q_2^\dagger)|}{\sqrt{|\det(1 + Q_1 Q_2^\dagger)(1 + Q_2 Q_1^\dagger)|}} = |\det(U_1^\dagger U_2 + V_1^\dagger V_2)|. \quad (\text{B24})$$

We first calculate the far field contribution and see that it exhibits from a similar logarithmic divergence as the boson mean field wave functions. Asymptotically far from the cores, whose sizes are given by ξ , one can diagonalize Eq. (B22) using a constant order parameter $\varphi_i = \Delta e^{i\phi}$. The solution of Eq. (B22) yields

$$U_k^2 = \frac{1}{2} \left(1 + \frac{\zeta_k}{\sqrt{\zeta_k^2 + \Delta^2}} \right), \quad (\text{B25})$$

$$V_k^2 = \frac{1}{2} \left(1 - \frac{\zeta_k}{\sqrt{\zeta_k^2 + \Delta^2}} \right) e^{i2\phi}, \quad (\text{B26})$$

with $\zeta_k = \hbar^2(k^2 - k_F^2)/2m$. Factorizing the determinant into blocks, as shown in Fig. 4, we obtain

$$W = W_{\text{core}} + \sum_{r_l > r_0} A_l w_l^{\text{far}},$$

$$w_l^{\text{far}} \simeq [1 - \cos(\phi_{1,l} - \phi_{2,l})] \int \frac{d^2k}{(2\pi)^2} U_k^2 V_k^2. \quad (\text{B27})$$

Summing over the far field blocks

$$\sum_l A_l [1 - \cos(\phi_{1,l} - \phi_{2,l})] \simeq \frac{1}{2} \int_{|\mathbf{x}| \gg r_0, d} d^2x (\nabla \phi \cdot \mathbf{d})^2 \quad (\text{B28})$$

one obtains

$$W \simeq \frac{1}{2} \pi n_{\text{eff}} d^2 \ln(R/r_0) + W_{\text{core}}, \quad (\text{B29})$$

where $n_{\text{eff}} = k_F / 4\pi\xi < n_e$.

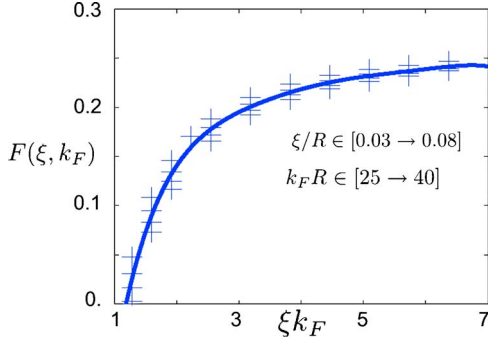


FIG. 8. (Color online) The function $F(k_F, \xi)$ defined in Eq. (B30), which yields the coefficient of the core contribution to the BCS vortex overlap on the sphere. k_F is the Fermi wave vector and ξ is Pippard's coherence length. The numerical data in the specified ranges of k_FR and ξ/R collapse to a function of the product ξk_F .

The divergence of the first term with $\log(R)$ arises from the far-field contributions. Again, it is an artifact of the BCS wave function, which is a mean field state where the condensate phase does not fluctuate. As for Bose coherent states, the BCS wave function also has a nonvanishing structure factor at zero momentum, and thus an infinite compressibility at zero temperature. This divergence is cancelled by including (RPA) phase fluctuations, which restores a finite zero temperature compressibility given by the density of states at the Fermi energy.

Here we are interested in the core contribution W_{core} of Eq. (B29). This requires a full diagonalization of the BdG equations. For the antipodal vortex pair on the sphere, the details of the computation are found in Appendix C. A fit to the numerically obtained values of W in Eq. (B24) yields the asymptotic expressions at large R/d :

$$W^{\text{BCS}} \simeq d^2 \left(\frac{k_F}{8\xi} \ln(R/\xi) + k_F^2 F(k_F \xi) \right) + O(d^4), \quad (\text{B30})$$

where F is a dimensionless function of order 0.2, of the scaling variable $(k_F \xi)$ as demonstrated by the collapse of the numerical data for W in Fig. 8.

The first R -dependent term is the diverging far field contributions discussed earlier, which is an artifact of the infinite compressibility of the BCS wave function. The second term is the core contribution which is in fact very large: it goes as $(k_F d)^2$. Thus we find that the core contribution effectively suppresses energy conserving tunneling between sites separated by more than a few Fermi wavelengths. In the regime of large coherence length relative to the mean free path, vortices could be dissipatively dragged by the bias current by exciting low energy core states⁵⁸. This, in essence, is the source of friction in Bardeen-Stephen flux creep theory.⁵⁹ This ‘‘frictional’’ motion involves impurity scattering inside the vortex cores,^{60,61} which we do not treat in this paper.

APPENDIX C: CALCULATIONS ON THE SPHERE

An antipodal vortex pair field can be expanded as

$$\varphi(\theta, \phi) = \sum_{l=1}^{\infty} \tilde{\varphi}_l Y_{l,1}(\theta, \phi), \quad (\text{C1})$$

where $Y_{lm}(\theta, \phi)$ are normalized spherical harmonics. Equation (C1) is an eigenfunction of $L^z = -i\hbar \partial_\phi$. The coherence length ξ determines the core sizes at the north and south poles, and thus the decay rate of the $\tilde{\varphi}_l$ with l .

The angular momentum representation, with a cutoff at $l_{\text{max}} \gg (R/\xi)$, reduces the Bogoliubov equations (B6) and (B22) to finite matrix diagonalizations. We can also translate the vortex wave functions using $SU(2)$ rotation $D_{mm'}^l$ matrices.

1. BEC with antipodal vortex pair

For the BEC vortex pair, some straightforward but tedious algebra can bring the overlap exponent in Eq. (B16) into a computationally convenient form

$$W_0 = \text{Re}[(\varphi_1^* U_1 - \varphi_1 V_1) S_{12}^{-1} [U_2^\dagger (\varphi_2 - \varphi_1) - V_2^\dagger (\varphi_2^* - \varphi_1^*)]],$$

$$W_1 = \frac{1}{2} \ln \det[S_{12}],$$

$$S_{12} = U_1^\dagger U_2 - V_1^\dagger V_2. \quad (\text{C2})$$

For the vortex pair field $\tilde{\varphi}$ given by Eq. (C1) the BdG equation possesses axial symmetry which allows $m = \bar{m}_n$ to be a good quantum number. The BdG eigenvectors have components given by

$$U_{l,m}^n = U_l^n \delta_{m,m_n},$$

$$V_{l,m}^n = V_l^n \delta_{m,m_n-2},$$

$$\delta_{nn'} = \sum_l U_l^n U_l^{n'} - V_l^n V_l^{n'} \quad (\text{C3})$$

for these coefficients are

$$E_n \begin{pmatrix} U^n \\ -V^n \end{pmatrix} = \begin{pmatrix} H^N & A \\ -A^\dagger & -H^N \end{pmatrix} \begin{pmatrix} U^n \\ -V^n \end{pmatrix}, \quad (\text{C4})$$

$$H^N(m) = \frac{\hbar^2}{2mR^2} l(l+1) \delta_{ll'} + V_{ll',m},$$

$$V_{ll',m} = \langle l, m | V_{\text{pin}}(\theta) + 2g|\tilde{\varphi}|^2 - \mu | l', m \rangle,$$

$$A_{ll'}(m) = g \langle l, m | \tilde{\varphi}^2 | l', m-2 \rangle, \quad (\text{C5})$$

where Eq. (C8) can be used for the precise numerical evaluation of the matrix elements.

2. Boson ground state overlap

Having determined U_l^n, V_l^n , and recognizing that the transformation between $\varphi_0, U_0 \cdot V_0$ and $\varphi_1, U_1 \cdot V_1$ simply involves an $O(3)$ rotation of the z axis by an angle θ , the overlap (C2) is given by

$$\begin{aligned}
 \langle \Phi_1 | \Phi_2 \rangle &= \det^{-1/2} [S] \exp[\vec{\varphi}^\dagger I S^{-1} J \vec{\varphi}], \\
 S_{nn'} &= \sum_l (U_l^n D_{m_n, m_n'}^l U_l^{n'} - V_l^n D_{m_n, m_n'}^l V_l^{n'}), \\
 I_{l,n} &= (U_l^n + V_l^n) \delta_{m_n, 1}, \\
 J_{n,l} &= U_l^n (\delta_{m_n, 1} - D_{m_n, 1}^l) + V_l^n (\delta_{m_n, 1} - D_{m_n, -2, -1}^l), \\
 \vec{\varphi}_l &= \int d\Omega Y_{l,1}^*(\theta, \phi) \varphi(\theta, \phi). \quad (\text{C6})
 \end{aligned}$$

It is easy to verify that for the limit $U_l^n = \delta_{n,l}, V_l^n = 0$, Eq. (C6) reduces to the result for free particles.

3. Fermions on a sphere

A polar vortex pair field described by Eq. (C1) defines the pairing order parameter

$$\Delta = \tilde{\varphi}(\theta, \phi) \quad (\text{C7})$$

by normalizing it such that $\sqrt{n_0} = \Delta_0$. In the spherical harmonic basis $|l, m\rangle$ the Hamiltonian (B22) simplifies greatly. The Laplacian is proportional to the diagonal operator L^2 , and nondiagonal matrix elements of functions $F(\theta, \phi)$ can be computed using $3j$ Racah coefficients.⁶²

$$\begin{aligned}
 \langle l, m | F | l', m - M \rangle &= \sum_{L, M} F_{LM} \left[\frac{(2l+1)(2L+1)(2l'+1)}{4\pi} \right]^{1/2} \\
 &\times (-1)^m \begin{pmatrix} l & L & l' \\ -m & M & m - M \end{pmatrix} \begin{pmatrix} l & L & l' \\ 0 & 0 & 0 \end{pmatrix}, \\
 F_{LM} &\equiv \int d\Omega Y_{L,M}^*(\Omega) F(\Omega). \quad (\text{C8})
 \end{aligned}$$

Due to axial symmetry, m is a good quantum number, which is to say that a function m_n is defined such that

$$\begin{aligned}
 U_{l,m}^n &= U_l^n \delta_{m, m_n}, \\
 V_{l,m}^n &= V_l^n \delta_{m', m_n - 1}. \quad (\text{C9})
 \end{aligned}$$

The matrix BdG equation for these coefficients is

$$\begin{aligned}
 E_n \begin{pmatrix} U^n \\ V^n \end{pmatrix} &= \begin{pmatrix} H^N & A \\ A^\dagger & -H^N \end{pmatrix} \begin{pmatrix} U^n \\ V^n \end{pmatrix}, \\
 H^N &= \left(\frac{\hbar^2}{2mR^2} l(l+1) - \varepsilon_F \right) \delta_{ll'}, \\
 A_{ll'} &= \langle l, m | \tilde{\varphi} | l', m - 1 \rangle. \quad (\text{C10})
 \end{aligned}$$

The overlap of two vortex pair states relatively rotated by θ is

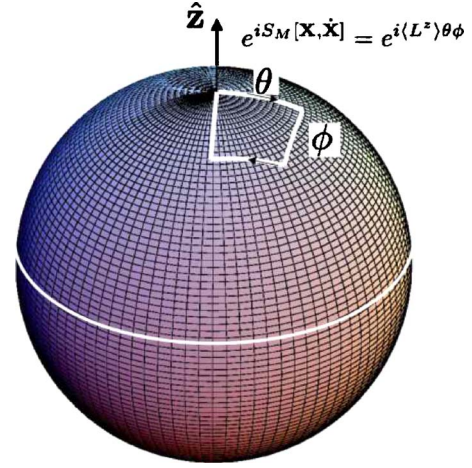


FIG. 9. (Color online) The orbit of a vortex pair on the sphere which is used to calculate the vortex Berry phase and Magnus action. Motion of the antipodal vortex pair is achieved by four successive rotations of the north pole, covering a solid angle of $\theta \times \phi$.

$$\langle \Phi_1 | \Phi_2 \rangle = \det_{nn'} \left[\sum_l (U_l^n D_{m_n, m_n'}^l U_l^{n'} + V_l^n D_{m_n - 1, m_n' - 1}^l V_l^{n'}) \right], \quad (\text{C11})$$

where $D_{mm'}^l(\theta)$ is the orthogonal rotation matrix.

APPENDIX D: THE MAGNUS ACTION

The calculation of the Berry phase for the motion of a vortex wave function can be done using the method of Arovas, Schrieffer, and Wilczek,⁶³ originally for quantum Hall effect quasiparticles, and later applied *mutatis mutandis* to superfluid vortices by Haldane and Wu.⁶⁴ Here we show how the Berry phase is calculated simply and exactly on a spherical geometry.

The spherical geometry yields many advantages for vortex wave functions. The geometric phase of a moving vortex is tricky to evaluate for superfluids and superconductors on a finite plane, since it sensitively depends on the boundary conditions. On the sphere, there are no boundaries to worry about. The translations are implemented by $O(3)$ rotations, whose generators do not commute. Hence we can show that the Magnus density of a general many-body wave function is simply given by the expectation value of angular momentum density. When applied to an antipodal vortex pair state, this result agrees with Thouless, Ao, and Niu's conclusion²⁷ that the Magnus density of a single vortex is just the superfluid density away from the vortex cores.

Consider a general many body wave function $|\Psi_0\rangle$ defined on a sphere of radius R , and calculate the Berry phase acquired by an infinitesimal loop of area $A = R\delta\theta \cdot R\delta\phi$ in parameter space, as depicted by Fig. 9.

The infinitesimal loop is divided into four segments $\langle i, i+1 \rangle$ such that the loop Berry phase is

$$e^{iS_M/\hbar} \simeq \prod_{i=0}^3 \langle \psi_{i+1} | \psi_i \rangle. \quad (\text{D1})$$

For a general wave function, the loop can be defined by a succession of small $O(3)$ rotations of a vector passing

through a special point on the sphere. For our purpose, we pick that point to be the vortex center. For a general wave function, however, the choice of special point is somewhat arbitrary. Inversely, for a given sequence of small rotations, each point on the sphere executes an orbit. The special points on the sphere which characterize the sequence are the two antipodal points whose loops have a maximal area (see Fig. 9). Without loss of generality, we choose to place these points at the north and south poles, and apply the corresponding sequence of rotations:

$$\begin{aligned} |\psi_1\rangle &= e^{iL_y\delta\theta/\hbar}|\psi_0\rangle, \\ |\psi_2\rangle &= e^{iL_x\delta\phi/\hbar}e^{iL_y\delta\theta/\hbar}|\psi_0\rangle, \\ |\psi_3\rangle &= e^{-iL_y\delta\theta/\hbar}e^{iL_x\delta\phi/\hbar}e^{iL_y\delta\theta/\hbar}|\psi_0\rangle, \\ |\psi_4\rangle &= |\psi_0\rangle. \end{aligned} \quad (\text{D2})$$

The overlaps upto quadratic order in $\delta\theta$ and $\delta\phi$ are found to be

$$e^{iS_M/\hbar} \approx 1 - i\delta\theta\delta\phi\langle L_z \rangle/\hbar + \dots, \quad (\text{D3})$$

where the expectation values are in the state $|\psi_0\rangle$.

Generalizing to a complete path, we obtain

$$S_M = - \int dt \langle \psi_0(t) | L | \psi_0(t) \rangle \frac{d\boldsymbol{\omega}}{dt}, \quad (\text{D4})$$

where the vector $\boldsymbol{\omega}$ is the rate of change of the solid angle, instantaneously directed toward the vortex core.

This Magnus action applies to any wave function, regardless of its correlations (e.g., superfluid, Fermi liquid, or solid). For an antipodal vortex pair in a superfluid, the angular momentum density is given by \hbar times the condensate number density n_0 , if one assumes that the thermal excitations (normal component) carry no angular momentum. Representing the vortex center coordinates by (X, Y) yields the Magnus Lagrangian

$$\mathcal{L}_M = 2\pi\hbar n_0 X\dot{Y}, \quad (\text{D5})$$

which resembles the effect of a uniform magnetic field in the z direction.

The fluctuations correction of the Bogoliubov corrected wave function (16) is given by

$$\mathcal{L}_M = 2\pi\hbar(n_0 + \bar{\delta n})X\dot{Y}. \quad (\text{D6})$$

Interestingly, although $\delta l_z(x) \neq \delta n(x)$, the system averaged quantities are found to be numerically equal, $\bar{\delta n} = \bar{\delta l}_z$. Equation (D6) yields Eq. (32) of the main text, if we define $n_s = n_0 + \bar{\delta n}$

*Present address: Department of Physics, Indian Institute of Technology at Delhi, New Delhi 110016, India.

- ¹P. W. Anderson, Rev. Mod. Phys. **38**, 298 (1966).
- ²M. Tinkham, *Introduction to Superconductivity* (Krieger, New York, 1980).
- ³V. Ambegaokar, B. I. Halperin, D. R. Nelson, and E. D. Siggia, Phys. Rev. B **21**, 1806 (1980).
- ⁴P. W. Anderson and Y. B. Kim, Rev. Mod. Phys. **36**, 39 (1964).
- ⁵G. Blatter, V. B. Geshkenbein, and V. M. Vinokur, Phys. Rev. Lett. **66**, 3297 (1991); P. Ao and D. J. Thouless, *ibid.* **70**, 2158 (1993); M. J. Stephen, *ibid.* **72**, 1534 (1994).
- ⁶U. Eckern and A. Schmid, Phys. Rev. B **39**, 6441 (1989); U. Eckern and E. B. Sonin, *ibid.* **47**, 505 (1993); R. Fazio, A. van Otterlo, and G. Schön, Europhys. Lett. **25**, 453 (1994); R. Iengo and G. Jug, Phys. Rev. B **52**, 7537 (1995).
- ⁷D. Ephron, A. Yazdani, A. Kapitulnik, and M. R. Beasley, Phys. Rev. Lett. **76**, 1529 (1996); J. B. Majer, J. Peguiron, M. Grifoni, M. Tsuvel, and J. E. Mooij, *ibid.* **90**, 056802 (2003).
- ⁸A. J. J. van Dalen, R. Griessen, S. Libbrecht, Y. Bruynseraede, and E. Osquiguil, Phys. Rev. B **54**, 1366 (1996); F. Tafuri, J. R. Kirtley, P. G. Medaglia, P. Orgiani, and G. Balestrino, Phys. Rev. Lett. **92**, 157006 (2004).
- ⁹M. P. A. Fisher, T. A. Tokuyasu, and A. P. Young, Phys. Rev. Lett. **66**, 2931 (1991).
- ¹⁰M. P. A. Fisher and D. H. Lee, Phys. Rev. B **39**, 2756 (1989); M. P. A. Fisher, Phys. Rev. Lett. **65**, 923 (1990); E. Shimshoni, A. Auerbach, and A. Kapitulnik, Phys. Rev. Lett. **80**, 3352 (1998).
- ¹¹A. F. Hebard and M. A. Paalanen, Phys. Rev. Lett. **65**, 927 (1990); A. Yazdani and A. Kapitulnik, *ibid.* **74**, 3037 (1995); D.

- Ephron, A. Yazdani, A. Kapitulnik, and M. R. Beasley, *ibid.* **76**, 1529 (1996).
- ¹²G. Sambandamurthy, L. W. Engel, A. Johansson, and D. Shahar, Phys. Rev. Lett. **92**, 107005 (2004); M. A. Steiner, G. Boebinger, and A. Kapitulnik, *ibid.* **94**, 107008 (2005).
- ¹³D. Dalidovich and P. Phillips, Phys. Rev. B **64**, 052507 (2001); V. M. Galitski, G. Refael, M. P. A. Fisher, and T. Senthil, Phys. Rev. Lett. **95**, 077002 (2005).
- ¹⁴G. Volovik, JETP Lett. **62**, 65 (1995).
- ¹⁵Q. Niu, P. Ao, and D. J. Thouless, Phys. Rev. Lett. **72**, 1706 (1994); **75**, 975 (1995).
- ¹⁶J. M. Duan, Phys. Rev. B **48**, 333 (1993); **49**, 12381 (1994); **75**, 974 (1995).
- ¹⁷E. Simanek, *Inhomogeneous Superconductors* (Oxford University Press, New York, 1994).
- ¹⁸D. P. Arovas and J. A. Freire, Phys. Rev. B **55**, 1068 (1997).
- ¹⁹E. B. Sonin, Zh. Eksp. Teor. Fiz. **64**, 970 (1973); [Sov. Phys. JETP **37**, 494 (1974)]; E. B. Sonin, Physica B **210**, 234 (1995).
- ²⁰This approach has been used to calculate tunneling rates of fractionally charged quasiparticles in the quantum Hall phase: A. Auerbach, Phys. Rev. Lett. **80**, 817 (1998); E. Shopen, Y. Gefen, and Y. Meir, Phys. Rev. Lett. **95**, 136803 (2005).
- ²¹A. Mizel, Phys. Rev. B **73**, 174502 (2006).
- ²²Y. J. Uemura *et al.*, Phys. Rev. Lett. **62**, 2317 (1989).
- ²³V. Ambegaokar, B. I. Halperin, and J. S. Langer, Phys. Rev. B **4**, 2612 (1971).
- ²⁴O. Viehweger and K. B. Efetov, J. Phys.: Condens. Matter **2**, 7049 (1990); S. C. Zhang, S. Kivelson, and D. H. Lee, Phys. Rev. Lett. **69**, 1252 (1992); Y. Imry, *ibid.* **71**, 1868 (1993); L.

- Zheng and H. A. Fertig, *ibid.* **73**, 878 (1994); O. Entin-Wohlman, A. G. Aronov, Y. Levinson, and Y. Imry, *ibid.* **75**, 4094 (1995).
- ²⁵D. Shahar, D. C. Tsui, M. Shayegan, E. Shimshoni, and S. L. Sondhi, *Science* **274**, 589 (1996); M. Hilke, D. Shahar, S. H. Song, D. C. Tsui, Y. H. Xie, and D. Monroe, *Nature (London)* **395**, 675 (1998).
- ²⁶E. Shimshoni and A. Auerbach, *Phys. Rev. B* **55**, 9817 (1997); E. Shimshoni, A. Auerbach, and A. Kapitulnik, *Phys. Rev. Lett.* **80**, 3352 (1998).
- ²⁷D. J. Thouless, Ping Ao, and Qian Niu, *Phys. Rev. Lett.* **76**, 3758 (1996).
- ²⁸A standard example of the Heitler-London approach can be found in D. C. Mattis, *Theory of Magnetism I* (Springer-Verlag, Berlin, 1988), Chap. 2.2.
- ²⁹Caution must be exercised using that Heitler-London method. Since both symmetric and antisymmetric energies are variational, their difference is neither an upper nor a lower bound on the exact tunnel splitting.
- ³⁰L. Onsager, *Nuovo Cimento, Suppl.* **6**, 249 (1949); R. P. Feynman and M. Cohen, *Phys. Rev.* **102**, 1189 (1956).
- ³¹L. P. Pitaevskii and S. Stringari, *Bose-Einstein Condensation* (Clarendon Press, Oxford, 2003).
- ³²We thank Ehud Altman and Anatoly Polkovnikov for alerting us to the spurious Anderson Overlap Catastrophe associated with coherent states.
- ³³E. P. Gross, *Nuovo Cimento* **20**, 454 (1961).
- ³⁴L. P. Pitaevskii, *Zh. Eksp. Teor. Fiz.* **40**, 646 (1961) [*Sov. Phys. JETP* **13**, 451 (1961)].
- ³⁵For example, see: A. L. Fetter and A. S. Svidzinsky, *J. Phys.: Condens. Matter* **13**, R135 (2001); S. Ghosh, *Phase Transitions* **77**, 625 (2004).
- ³⁶C. Pethick and H. Smith, *Bose-Einstein Condensation in Dilute Gases* (Cambridge University Press, Cambridge, 2002), Chap. 9.
- ³⁷The relevant time scale for tunneling is the time to move in the inverted potential barrier for the instanton action, which is of the order of \hbar/\bar{V} .
- ³⁸T. Holstein, *Ann. Phys. (N.Y.)* **8**, 343 (1959); A. Miller and E. Abrahams, *Phys. Rev.* **120**, 745 (1960); G. D. Mahan, *Many Particle Physics* (Plenum, New York, 1986).
- ³⁹N. F. Mott, *Philos. Mag.* **19**, 835 (1969).
- ⁴⁰B. I. Shklovskii, *Zh. Eksp. Teor. Fiz.* **36**, 43 (1982) [*Sov. Phys. JETP* **36**, 51 (1982)].
- ⁴¹M. M. Fogler, A. Yu. Dobin, and B. I. Shklovskii, *Phys. Rev. B* **57**, 4614 (1998).
- ⁴²The two limits do not necessarily commute, as known for Anderson insulators where quantum interference causes localization. Here we are interested in a strongly dephased system at finite temperatures. We thank Misha Fogler for a clarifying discussion.
- ⁴³T. Holstein, *Phys. Rev.* **124**, 1329 (1961).
- ⁴⁴V. J. Goldman, M. Shayegan, and D. C. Tsui, *Phys. Rev. Lett.* **61**, 881 (1988); R. L. Willett, H. L. Stormer, D. C. Tsui, L. N. Pfeiffer, K. W. West, and K. W. Baldwin, *Phys. Rev. B* **38**, 7881 (1988).
- ⁴⁵D. J. Bergman and D. Stroud, *Solid State Phys.* **46**, 147 (1992); A. M. Dykhne and I. M. Ruzin, *Phys. Rev. B* **50**, 2369 (1994).
- ⁴⁶L. P. Pryadko and A. Auerbach, *Phys. Rev. Lett.* **82**, 1253 (1999).
- ⁴⁷D. R. Hofstadter, *Phys. Rev. B* **14**, 2239 (1976).
- ⁴⁸L. Balents, L. Bartosch, A. Burkov, S. Sachdev, and K. Sengupta, *Phys. Rev. B* **71**, 144508 (2005).
- ⁴⁹M. R. Matthews, B. P. Anderson, P. C. Haljan, D. S. Hall, C. E. Wieman, and E. A. Cornell, *Phys. Rev. Lett.* **83**, 2498 (1999); K. W. Madison, F. Chevy, W. Wohlleben, and J. Dalibard, *ibid.* **84**, 806 (2000); J. R. Abo-Shaeer *et al.*, *Science* **292**, 476 (2001); E. Hodby, G. Hechenblaikner, S. A. Hopkins, O. M. Marago, and C. J. Foot, *Phys. Rev. Lett.* **88**, 010405 (2002).
- ⁵⁰M. Franz, Z. Tesanovic, and O. Vafek, *Phys. Rev. B* **66**, 054535 (2002).
- ⁵¹E. Altman and A. Auerbach, *Phys. Rev. B* **65**, 104508 (2002).
- ⁵²P. Nikolic and S. Sachdev, *Phys. Rev. B* **73**, 134511 (2006).
- ⁵³J. Clayhold, N. P. Ong, Z. Z. Wang, J. M. Tarascon, and P. Barbois, *Phys. Rev. B* **39**, 7324 (1989); H. Y. Hwang, B. Batlogg, H. Takagi, H. L. Kao, J. Kwo, R. J. Cava, J. J. Krajewski, and W. F. Peck, *Phys. Rev. Lett.* **72**, 2636 (1994).
- ⁵⁴F. F. Balakirev *et al.*, *Nature (London)* **424**, 912 (2003).
- ⁵⁵A. L. Fetter, *Phys. Rev. A* **53**, 4245 (1996).
- ⁵⁶Y. Castin, in *Coherent Atomic Matter Waves, Lecture Notes of Les Houches Summer School*, edited by R. Kaiser, C. Westbrook, and F. David (EDP Sciences and Springer-Verlag, Berlin, 2001).
- ⁵⁷J. Steinhauer, R. Ozeri, N. Katz, and N. Davidson, *Phys. Rev. Lett.* **88**, 120407 (2002); J. Steinhauer, N. Katz, R. Ozeri, N. Davidson, C. Tozzo, and F. Dalfovo, *ibid.* **90**, 060404 (2003).
- ⁵⁸C. Caroli, P. G. de Gennes, and J. Matricon, *Phys. Lett.* **9**, 307 (1964).
- ⁵⁹J. Bardeen and M. J. Stephen, *Phys. Rev.* **140**, A1197 (1965).
- ⁶⁰G. Blatter, M. V. Feigel'man, V. B. Geshkenbein, A. I. Larkin, and V. M. Vinokur, *Zh. Eksp. Teor. Fiz.* **57**, 699 (1993) [*JETP* **5**, 711 (1993)]; G. Blatter *et al.*, *Rev. Mod. Phys.* **66**, 1125 (1994); A. van Otterlo, M. Feigel'man, V. Geshkenbein, and G. Blatter, *Phys. Rev. Lett.* **75**, 3736 (1995).
- ⁶¹N. B. Kopnin, *Rep. Prog. Phys.* **65**, 1633 (2002).
- ⁶²A. R. Edmonds, *Angular Momentum in Quantum Mechanics* (Princeton University Press, Princeton, 1996).
- ⁶³D. Arovas, J. R. Schrieffer, and F. Wilczek, *Phys. Rev. Lett.* **53**, 722 (1984).
- ⁶⁴F. D. M. Haldane and Y.-S. Wu, *Phys. Rev. Lett.* **55**, 2887 (1985).